

Kinetic plasma turbulence: recent insights and open questions from 3D3V simulations

Silvio Sergio Cerri^{1,*}, Daniel Grošelj², Luca Franci³

¹Department of Astrophysical Sciences, Princeton University, Princeton, NJ, USA;

²Max-Planck-Institute for Plasma Physics, Garching, Germany

³School of Physics and Astronomy, Queen Mary University of London, London, UK;

Correspondence*:

Peyton Hall, 4 Ivy Ln, Princeton, NJ 08544, USA
scerri@astro.princeton.edu

ABSTRACT

Turbulence and kinetic processes in magnetized space plasmas have been extensively investigated over the past decades via *in-situ* spacecraft measurements, theoretical models and numerical simulations. In particular, multi-point high-resolution measurements from the *Cluster* and *MMS* space missions brought to light an entire new world of processes, taking place at the plasma kinetic scales, and exposed new challenges for their theoretical interpretation. A long-lasting debate concerns the nature of ion and electron scale fluctuations in solar-wind turbulence and their dissipation via collisionless plasma mechanisms. Alongside observations, numerical simulations have always played a central role in providing a test ground for existing theories and models. In this Perspective, we discuss the advances achieved with our 3D3V (reduced and fully) kinetic simulations, as well as the main questions left open (or raised) by these studies. To this end, we combine data from our recent kinetic simulations of both freely decaying and continuously driven fluctuations to assess the similarities and/or differences in the properties of plasma turbulence in the sub-ion range. Finally, we discuss possible future directions in the field and highlight the need to combine different types of numerical and observational approaches to improve the understanding of turbulent space plasmas.

Keywords: magnetic fields, plasma turbulence, solar wind, kinetic plasma simulations, turbulence intermittency, plasma waves

1 INTRODUCTION

With the establishment of satellite space missions, the near-Earth environment and the solar wind have provided unique opportunities to explore the physics of weakly collisional, magnetized plasmas (e.g., Bruno and Carbone, 2013; Chen, 2016; Verscharen et al., 2019). In particular, increasingly accurate *in-situ* measurements of plasma fluctuations and particle distribution functions from *Cluster* and *MMS* have uncovered an entire new world of kinetic processes occurring in plasma turbulence (e.g., Alexandrova et al., 2009, 2012, 2013; Sahraoui et al., 2009, 2010; Chen et al., 2010, 2019; Greco et al., 2016; Narita et al., 2016; Chasapis et al., 2017; Chen and Boldyrev, 2017; Huang et al., 2017; Roberts et al., 2017; Servidio et al., 2017). These observations highlight a change in the turbulent cascade at plasma microscales, challenging the community for a consistent theory of kinetic-range turbulence. In fact, several collisionless plasma processes may be simultaneously at play and compete with each other in determining the nature of ion-scale and electron-scale fluctuations (e.g., Stawicki et al., 2001; Galtier and Bhattacharjee, 2003; Howes

et al., 2008a; Gary and Smith, 2009; Schekochihin et al., 2009; He et al., 2012; Podesta, 2012; Boldyrev and Perez, 2012; Boldyrev et al., 2013; Matthaeus et al., 2014; Passot and Sulem, 2015, 2019; Kunz et al., 2018; Passot et al., 2018) and, consequently, how free energy cascades in phase space (e.g., Schekochihin et al., 2008; Servidio et al., 2017; Adkins and Schekochihin, 2018; Cerri et al., 2018; Eyink, 2018; Pezzi et al., 2018; Kawazura et al., 2019). Many observations at ion and sub-ion scales, specifically, suggest that turbulent fluctuations exhibit properties mainly typical of kinetic Alfvén waves (KAWs) (Leamon et al., 1998; Sahraoui et al., 2009; Podesta and TenBarge, 2012; Salem et al., 2012; Chen et al., 2013; Chen, 2016; Kiyani et al., 2013; Lacombe et al., 2017). The emergence of KAW-like fluctuations in kinetic turbulence has been also supported by means of a large number of theoretical and numerical works (e.g., Hollweg, 1999; Stawicki et al., 2001; Gary and Nishimura, 2004; Howes et al., 2008a; Gary and Smith, 2009; Sahraoui et al., 2012; TenBarge et al., 2012; Vásconez et al., 2014, 2015; Franci et al., 2015; Cerri et al., 2016; Pucci et al., 2016; Zhao et al., 2016; Valentini et al., 2017; Grošelj et al., 2019). Some of these studies rely on the so-called spectral field ratios, which provide a measure of the wave-like polarization properties of the turbulent fluctuations, as compared to what linear theory predicts (see, e.g., Boldyrev et al., 2013, and Sec. 3).

In the above context, direct numerical simulations play a key role by providing a controlled test ground for different theories, providing information not accessible to observations. Enormous efforts have been recently made to understand 3D kinetic turbulence via numerical experiments (e.g., Howes et al., 2008b; Gary et al., 2012; TenBarge and Howes, 2013; Vasquez et al., 2014; Servidio et al., 2015; Told et al., 2015; Wan et al., 2015, 2016; Bañón Navarro et al., 2016; Comişel et al., 2016; Cerri et al., 2017b, 2018; Hughes et al., 2017a; Kobayashi et al., 2017; Hughes et al., 2017b; Franci et al., 2018b,a; Grošelj et al., 2018; Arzamasskiy et al., 2019; Roytershteyn et al., 2019; Zhdankin et al., 2019; Grošelj et al., 2019). In this Perspective, we combine data from our recent 3D3V studies (Cerri et al., 2017b; Franci et al., 2018b; Grošelj et al., 2019) to investigate whether common turbulence features exist in all three independently performed simulations (Sec. 2), thus indicating a certain “universality” of kinetic-scale turbulence. Moreover, we also highlight possible model-dependent differences between the 3D hybrid-kinetic and fully kinetic simulations. We mention that this approach follows the general idea of adopting different models (and/or implementations) to study turbulent heating and dissipation in collisionless plasmas that was initiated within the “Turbulent Dissipation Challenge” framework (Parashar et al., 2015). Here we extend similar comparative analysis of the spectral properties that have been previously performed in a reduced two-dimensional setup (see Cerri et al., 2017a; Franci et al., 2017; Grošelj et al., 2017) to the more realistic three-dimensional geometry (Sec. 3), and we present a new analysis of our data based on local structure functions (Sec. 4). Finally, we discuss possible implications for sub-ion-scale turbulence and future directions emerging from this study (Sec. 5).

2 DATA SETS

In the following, we consider three recent kinetic simulations in a six-dimensional phase space (“3D3V”) using: (i) CAMELIA, a hybrid particle-in-cell (PIC) code with massless electrons (Franci et al., 2018a), (ii) HVM, an Eulerian hybrid-Vlasov code with finite electron-inertia effects (Valentini et al., 2007), and (iii) OSIRIS, a fully kinetic PIC code (Fonseca et al., 2002, 2013). Unless otherwise specified, parallel (\parallel) and perpendicular (\perp) directions are defined with respect to the global mean magnetic field $\mathbf{B}_0 = B_0 \mathbf{e}_z$. Franci et al. (2018b) employed the CAMELIA code to investigate freely decaying, Alfvénic fluctuations in a cubic box ($L_{\parallel} = L_{\perp} = 128d_i$ with 512^3 grid points and 2048 particles per cell (ppc)) for $\beta_i = \beta_e = 0.5$, where $\beta_s = 8\pi n_0 T_s / B_0^2$ is the species beta. Cerri et al. (2017b) instead adopted the HVM code to study freely

decaying compressive fluctuations in an elongated box ($L_{\parallel} = 2L_{\perp} \simeq 63d_i$ with $384^2 \times 64$ grid points in real space, and 51^3 points in a velocity space bounded by $|v/v_{th,i}| \leq 5$) for $\beta_i = \beta_e = 1$ and with a reduced ion-electron mass ratio of $m_i/m_e = 100$ (viz. including d_e -effects in a generalized Ohm's law). Spectral filters were applied at runtime, determining a cutoff in the turbulent spectrum at $k_{\perp}d_i > 20$ and at $k_zd_i > 2$. Finally, Grošelj et al. (2019) use the OSIRIS code to investigate continuously driven Alfvénic fluctuations in a $\beta_i \approx \beta_e \approx 0.5$ plasma with $m_i/m_e = 100$. An elongated box was used ($L_{\parallel} = 2.56L_{\perp} \simeq 48.3d_i$ with $928^2 \times 1920$ grid points and 150 ppc per species). An example of $\delta\tilde{B}_{\perp} = \delta B_{\perp}/\delta B_{\perp}^{(\text{rms})}$ in a two-dimensional cut perpendicular to \mathbf{B}_0 is given in Fig. 1(a), along with a schematic representation of these simulations in the $(k_{\perp}, k_{\parallel})$ plane (Fig. 1(b)).

In the following, the analysis of freely decaying simulations (viz., CAMELIA and HVM) is performed at the peak of the turbulent activity (cf., e.g., Servidio et al., 2015), while for the continuously driven OSIRIS run we consider the turbulence at the end of the simulation when the kinetic range spectra appear converged. Following Franci et al. (2018b) and Grošelj et al. (2019), PIC data have been filtered before performing the analysis to remove spectral regions dominated by particle noise. The OSIRIS data have been filtered for $k_{\perp}d_i > 30$ or $k_zd_i > 12$ and downsampled to a grid $464^2 \times 640$. Note that OSIRIS simulations require to resolve the Debye scale, while the physical scales of interest are well represented at a lower resolution. A short-time average over $\Delta t\Omega_{ce} = 2$ (Ω_{ce} being the electron cyclotron frequency) was also performed to further reduce electron-scale noise (Grošelj et al., 2019). The CAMELIA data have been filtered for $k_{\perp}d_i > 10$ or $k_zd_i > 2$. We also considered alternative filtering approaches confirming that our results are not very sensitive to such particular choice.

3 SPECTRAL SLOPES AND NORMALIZED FIELD RATIOS

Here we review and compare the standard set of spectral properties in our independently performed 3D kinetic simulations, namely the slopes of the turbulence power spectra and the spectral field ratios. Early theoretical predictions for sub-ion-range turbulence (e.g., Cho and Lazarian, 2004; Schekochihin et al., 2009) proposed a spectral scaling $\sim k_{\perp}^{-7/3}$ for the magnetic energy spectrum. However, solar wind observations typically exhibit much steeper magnetic spectra, namely $\sim k_{\perp}^{-2.8}$ (e.g., Alexandrova et al., 2009, 2013; Sahraoui et al., 2010; Chen, 2016; Kobayashi et al., 2017; Sorriso-Valvo et al., 2018). Similar spectral exponents were also reported in recent 3D kinetic simulations (Told et al., 2015; Cerri et al., 2017b, 2018; Franci et al., 2018a,b; Grošelj et al., 2018; Arzamasskiy et al., 2019; Grošelj et al., 2019). Recently, refined predictions were proposed to explain steeper spectra. Those include intermittency corrections (Boldyrev and Perez, 2012), dissipative effects (Howes et al., 2011; Passot and Sulem, 2015), and reconnection-mediated turbulence (Loureiro and Boldyrev, 2017; Mallet et al., 2017a). Further insight into the nature of kinetic-scale turbulence can be obtained from the spectral field ratios, which have been used to detect wave-like polarization properties in solar-wind turbulence and in kinetic simulations (e.g., Sahraoui et al., 2009; Salem et al., 2012; TenBarge et al., 2012; Chen et al., 2013; Kiyani et al., 2013; Cerri et al., 2017b; Franci et al., 2018b; Grošelj et al., 2018).

In Fig. 1(c) the two-dimensional Fourier spectra, $\mathcal{E}(k_{\perp}, k_z)$, are shown. The wavenumber region (k_{\perp}, k_z) occupied by the turbulent fluctuations already highlights the anisotropic nature of the cascade, with energy preferentially flowing to high k_{\perp} . However, note that the 2D Fourier spectrum may exhibit a weaker anisotropy than the one typical of turbulent eddies, which are elongated along the *local* field direction (see, e.g., Cho and Vishniac, 2000). We perform a local analysis of anisotropy in Sec. 4.1.

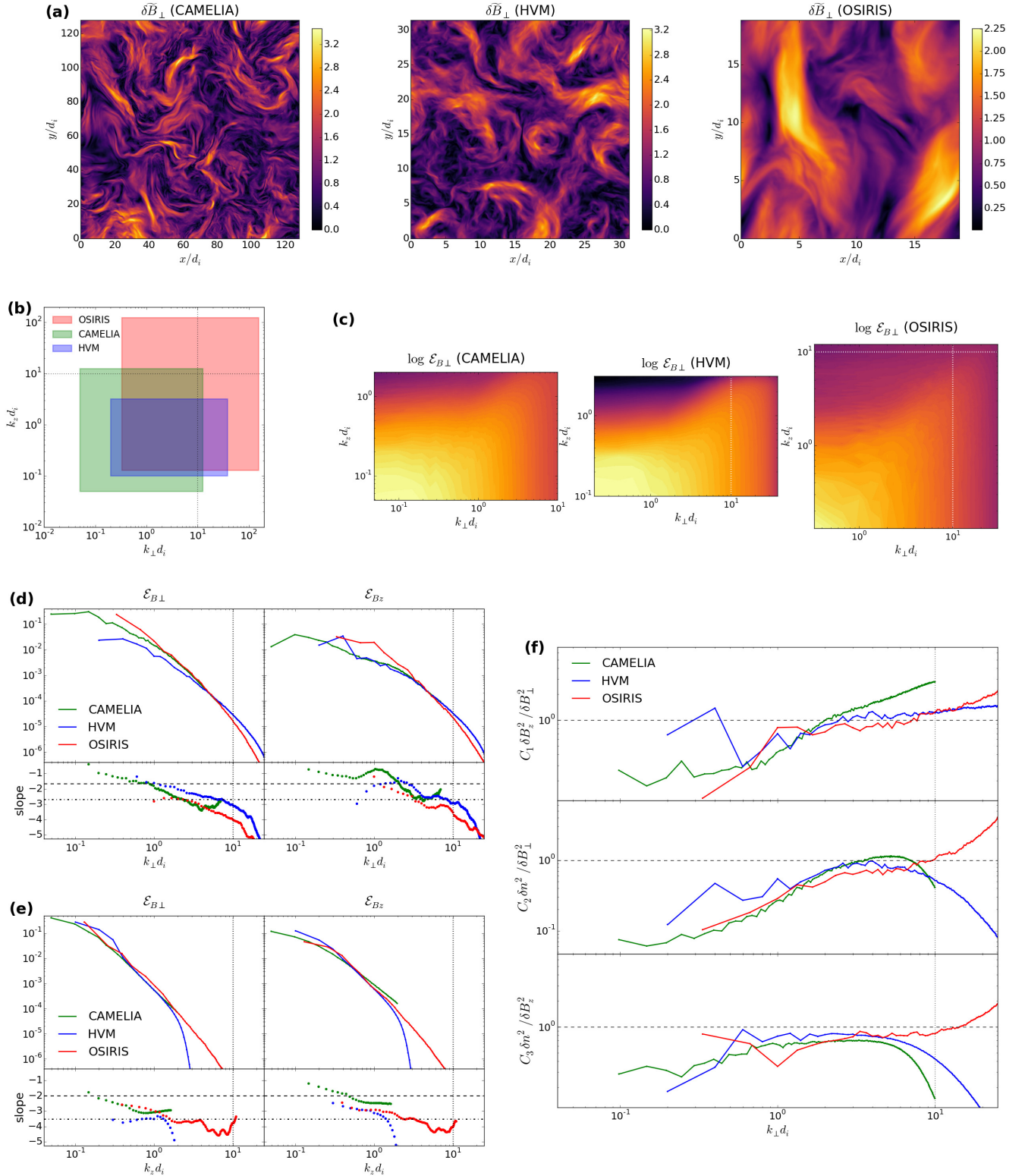


Figure 1. (a) $\delta \tilde{B}_\perp = \delta B_\perp / \delta B_\perp^{(\text{rms})}$ in a plane perpendicular to B_0 . (b) Nominal wavenumber-space representation of simulations. (c) δB_\perp spectrum in (k_\perp, k_z) space. White dotted lines mark $k d_e = 1$. (d) Top panels: reduced spectra versus $k_\perp d_i$. Spectra have been shifted (see text). Bottom panels: local spectral exponents. Horizontal lines denote $-5/3$ (dashed) and $-8/3$ (dash-dotted) slopes. Vertical dotted line marks $k_\perp d_e = 1$. (e) Same as (d), but versus $k_z d_i$. Here -2 (dashed) and $-7/2$ (dash-dotted) slopes are marked for reference. (f) Spectral ratios versus k_\perp , normalized to the asymptotic KAW prediction (dashed horizontal lines; see text for details).

In Fig. 1(d)–(e), the reduced 1D spectra, $\mathcal{E}(k_{\perp})$ (upper panels), and their local slope (lower panels) are reported. To remove the effects of different energy injection conditions, the k_{\perp} -spectra have been normalized so that they overlap in the sub-ion range, at $k_{\perp}d_i \simeq 5$. According to the spectral anisotropy in Fig. 1(c), the k_z -spectra have been consequently matched at $k_zd_i \simeq 0.5$. For our choice of low-pass filter (see Sec. 2), CAMELIA spectra artificially flatten beyond $k_{\perp}d_i \gtrsim 7$ due to PIC noise, and therefore we do not show CAMELIA data in this range in Fig. 1(d). Overall, the spectral slopes are consistent with each other, although the spectra obtained from the three simulations do not quite assume a universal shape. Close to the box scale, the spectral exponents are likely affected by the turbulence injection details. It is also possible that some of the sub-ion scale spectral exponents are not fully converged in terms of the box size (which was different for each simulation) and of the limited extent of sub-ion range itself. 3D3V simulations with a significantly larger sub-ion range are required to clarify this point. To some degree, differences at sub-ion scales could also be physical. In particular, the HVM simulation includes electron inertia effects in Ohm's law, while the OSIRIS results include the full electron kinetics, such as electron Landau damping and finite electron Larmor radius corrections. It is interesting to notice that OSIRIS spectra become steeper than the hybrid counterparts beyond $k_{\perp}d_i \gtrsim 3$, for our particular choice of the mass ratio ($m_i/m_e = 100$). This feature has been usually explained in terms of electron Landau damping (Grošelj et al., 2017; Chen et al., 2019), which is not included in the hybrid-kinetic model.

In Fig. 1(f), we report the comparison of spectral ratios, $C_1 \delta B_z^2 / \delta B_{\perp}^2$ (top), $C_2 \delta n^2 / \delta B_{\perp}^2$ (middle), and $C_3 \delta n^2 / \delta B_z^2$ (bottom). The ratios are normalized to the β -dependent kinetic Alfvén wave (KAW) eigenvalue from asymptotic linear theory ($\rho_i^{-1} \ll k_{\perp} \ll \rho_e^{-1}$ and $k_{\parallel} \ll k_{\perp}$), namely $C_1 = (2 + \beta)/\beta$, $C_2 = (2 + \beta)\beta/4$, and $C_3 = \beta^2/4$, where $\beta = \beta_i + \beta_e$ (see, e.g., Boldyrev et al., 2013, for details). In the normalized units, asymptotic KAW theory predicts a value of unity for all three ratios. This is essentially the result of KAWs developing a certain degree of magnetic compressibility at sub-ion scales, which sets the relation between δB_{\perp} and δB_{\parallel} , and requiring that compressive magnetic fluctuations are pressure balanced, which in turn provides a relation between δB_{\parallel} and δn (see, e.g., Schekochihin et al., 2009; Boldyrev et al., 2013). As found in previous studies (e.g., Salem et al., 2012; TenBarge et al., 2012; Chen et al., 2013; Cerri et al., 2017b; Franci et al., 2018b; Grošelj et al., 2018), the spectral field ratios are overall consistent with KAW-like turbulence at sub-ion scales. This is not completely surprising, as both in CAMELIA and OSIRIS simulations, Alfvénic fluctuations are injected. On the other hand, compressible magnetic fluctuations (i.e., including δB_{\parallel}) are injected in HVM run, and yet KAW-like fluctuations still develop. It was also proposed that KAWs may, quite generally, emerge as a result of Alfvén waves interacting with large-scale inhomogeneities (Pucci et al., 2016). Thus, the KAW-like spectral properties at sub-ion scales appear to be a relatively robust feature, independent of the details of the turbulent fluctuations injected at the MHD scales (cf. Cerri et al., 2017a). While the results are overall consistent, some differences are also seen, most notably in the high- k_{\perp} range ($k_{\perp}d_i \gtrsim 10$), which could be presumably attributed to various numerical artifacts. However, some deviations could also relate to differences between the hybrid-kinetic and fully kinetic model (for instance, some dispersion relation properties not being exactly the same (e.g., Told et al., 2016)).

So are the sub-ion-scale field polarizations indeed KAW-like? As discussed above, recent observations and kinetic simulations are consistent with such idea, although linear wave predictions are not necessarily satisfied precisely (e.g., Kiyani et al., 2013; Chen et al., 2013; Cerri et al., 2017b; Franci et al., 2018b). Chen et al. (2013) report an average value of 0.75 for the normalized ratio $C_2 \delta n^2 / \delta B_{\perp}^2$, whereas (asymptotic) KAW theory predicts a value of unity. That latter may be due to different reasons, among which we remark the following two: (i) sub-ion-range turbulence is not made of purely KAW-like fluctuations, and/or (ii) the

asymptotic conditions that are used in the derivation of linear theory predictions are not met exactly because of the limited sub-ion range of scales and/or because of the inherently nonlinear dynamics of turbulence. These two explanations are not mutually exclusive, of course. Indeed, sub-ion-scale turbulence can in principle include contributions from wave-like fluctuations of other nature. This may include fluctuations consistent with whistler (e.g., Gary and Smith, 2009), ion-cyclotron (e.g., Omidi et al., 2014; Zhao et al., 2018), or ion Bernstein waves (e.g., Podesta, 2012; Grošelj et al., 2017; Del Sarto et al., 2017), to name a few. On the other hand, the spectral ratios could also deviate from linear KAW predictions as a result of nonlinear dynamics. For example, Boldyrev et al. (2013) propose that, specifically the (normalized) $C_2 \delta n^2 / \delta B_{\perp}^2$ ratio may fall somewhat below the KAW prediction due to a (yet to be investigated) nonlinear effect, analogous to the residual-energy phenomenon in MHD turbulence.

4 MULTI-POINT STRUCTURE FUNCTIONS

Beyond energy spectra, fluctuations across different scales may be investigated in more detail via structure functions, i.e., the moments of local field increments (e.g., Frisch, 1995; Biskamp, 2008). Two-point structure functions, $S_m^{(2)}$ (m being the order), are most common. However, these cannot quantitatively produce the correct scaling for fluctuations with power spectra steeper than $\sim k^{-3}$, assuming a clean power-law spectrum (Falcon et al., 2007; Cho and Lazarian, 2009). Therefore, structure functions using more than two points are generally required at kinetic scales. Essentially, higher-order increments yield a scale decomposition that is more effective in filtering out the large-scale fluctuations below $k \approx \pi/\ell$ in spectral space, where ℓ is the increment scale. We also mention that if the signal is a polynomial of degree $\mathcal{N} - 2$, its corresponding 2nd-order, \mathcal{N} -point structure function vanishes (Cho, 2019). This makes multi-point structure functions more suitable for the analysis of relatively smooth signals with steep spectra (Schneider et al., 2004). A detailed review of \mathcal{N} -point increments, as well as their physical interpretation can be found in Cho (2019). Here, we consider for some field $f(\mathbf{x})$ the *conditional*, five-point structure functions:

$$S_m^{(5)}(\ell, \vartheta_{B_{\text{loc}}}) = \langle |\Delta f(\mathbf{x}, \ell)|^m | \ell, \vartheta_{B_{\text{loc}}} \rangle_{\mathbf{x}} \quad (1)$$

where $\Delta f(\mathbf{x}, \ell) = [f(\mathbf{x}+2\ell) - 4f(\mathbf{x}+\ell) + 6f(\mathbf{x}) - 4f(\mathbf{x}-\ell) + f(\mathbf{x}-2\ell)]/\sqrt{35}$ is the (normalized) field increment, $\langle \dots \rangle_{\mathbf{x}}$ is a space average, and $\vartheta_{B_{\text{loc}}}$ is the angle between the increment vector ℓ and the local mean magnetic field \mathbf{B}_{loc} . The term ‘‘conditional’’ implies that S_m are defined as conditional averages of $|\Delta f(\mathbf{x}, \ell)|^m$, using only those points in the statistical sample that fall within a given (narrow) range for ℓ and $\vartheta_{B_{\text{loc}}}$. We also considered three-point structure functions (see Fig. 2(a)) and, for a limited number of cases, seven-point structure functions (not shown). Comparison between the three-point, five-point and seven-point structure functions shows not only qualitative similarities among the three cases, but an apparent quantitative convergence with increasing number of points. We chose to illustrate the results in Fig. 2 in terms of five-point structure functions in order to provide better constraints for the theoretical predictions. Similar to two-point increments, where the local mean field is often defined as $\mathbf{B}_{\text{loc}}(\mathbf{x}, \ell) = [\mathbf{B}(\mathbf{x}) + \mathbf{B}(\mathbf{x}+\ell)]/2$ (e.g., Cho and Vishniac, 2000; Mallet et al., 2016), we obtain \mathbf{B}_{loc} by averaging over the points used for the increment. For five-point increments, a reasonable definition is $\mathbf{B}_{\text{loc}}(\mathbf{x}, \ell) = [\mathbf{B}(\mathbf{x}+2\ell) + 4\mathbf{B}(\mathbf{x}+\ell) + 6\mathbf{B}(\mathbf{x}) + 4\mathbf{B}(\mathbf{x}-\ell) + \mathbf{B}(\mathbf{x}-2\ell)]/16$. It is straightforward to check that such mean field definition filters out fluctuations around the scale of the increment $\sim \ell$, while preserving the contribution from scales larger than ℓ .

In what follows, we consider field-perpendicular, $S_m(\ell_\perp) \equiv S_m^{(5)}(\ell_\perp, 90^\circ - \Delta\vartheta \leq \vartheta_{B_{\text{loc}}} \leq 90^\circ)$, and field-parallel, $S_m(\ell_\parallel) \equiv S_m^{(5)}(\ell_\parallel, \vartheta_{B_{\text{loc}}} \leq \Delta\vartheta)$, five-point structure functions of the magnetic field and density fluctuations, where $\Delta\vartheta$ represents a finite angular tolerance used in practice to determine the *local* perpendicular and parallel directions. We reduce $\Delta\vartheta$ until the scalings appear converged. The field increments, from which we obtain the conditional structure functions, are evaluated at every grid point. In each grid point and at every scale, increments are sampled along random directions. The numbers of these random directions per grid point have been tested to provide a statistically significant (i.e., converged) sample. The sample that is used in the following is such that any structure function $S_m(\ell, \vartheta_{B_{\text{loc}}})$ counts at least 1.5×10^5 points per scale ℓ , in any given band for $\vartheta_{B_{\text{loc}}}$.

4.1 Spectral anisotropy

A delicate point concerns the sub-ion-range spectral anisotropy, $k_\parallel \sim k_\perp^\alpha$ (cf., e.g., Schekochihin et al., 2009; Boldyrev and Perez, 2012; Cerri et al., 2018; Landi et al., 2019). As is known from MHD, electron-MHD (EMHD), and kinetic-reduced-MHD (KRMHD) turbulence (Cho and Vishniac, 2000; Cho and Lazarian, 2009; Meyrand et al., 2019), the true anisotropy is often revealed only when measured with respect to the *local*, scale-dependent mean magnetic-field direction. Somewhat contradicting estimates, obtained with different methods, for the sub-ion-scale anisotropy have been presented in recent works. Here, we revisit this issue using the above-mentioned implementation of five-point structure functions, consistently applied to all data.

In Fig. 2(a) we show the perpendicular and parallel second-order structure function scalings, and in Fig. 2(b) we show the inferred anisotropy, $\ell_\parallel(\ell_\perp)$. The characteristic parallel length $\ell_\parallel(\ell_\perp)$ at a given perpendicular scale ℓ_\perp is obtained by finding the value of ℓ_\parallel , at which the amplitudes of $S_2(\ell_\parallel)$ and $S_2(\ell_\perp)$ match. To illustrate the sensitivity to the local mean field direction, we show in Fig. 2(a) the convergence with respect to the angular tolerance $\Delta\vartheta$. The parallel scalings appear converged at $\Delta\vartheta \simeq 3^\circ$ for CAMELIA data and at around $\Delta\vartheta \simeq 1.5^\circ$ for HVM, whereas the OSIRIS results are somewhat less sensitive to $\Delta\vartheta$ (converging already for $\Delta\vartheta \simeq 6^\circ$). This difference may occur because OSIRIS simulation exhibits the weakest anisotropy (in absolute values). Physically, $\Delta\vartheta$ should be approximately no larger than $\sim \ell_\perp/\ell_\parallel$ of the small-scale turbulent eddies. Thus, smaller $\Delta\vartheta$ are needed if a stronger anisotropy develops at the energy-containing scales.

All quantities seem to converge to a scaling close to $\ell_\parallel \sim \ell_\perp^{2/3}$ (although δB_\perp fluctuations in HVM exhibit a scaling closer to $1/3$ over the range of scales across $\ell_\perp \sim d_i (= \rho_i)$). It is worth noticing, however, that this is not the end of the story, as the scaling is not quite $2/3$ and additional effects such as B -field curvature may slightly change the anisotropy. Indeed, the field increments are taken along a straight line. If the local magnetic field lines are significantly curved over the extent of the increment stencil ($= 4\ell$ for five-point increments), the field increments will mix contributions from different field lines, in which case the anisotropy may be somewhat underestimated. It is worth mentioning that a scaling $\ell_\parallel \sim \ell_\perp^{2/3}$ was proposed in Boldyrev and Perez (2012), based on a filling-factor correction for the fluctuation energy. Assuming the energy is concentrated in intermittent, two-dimensional structures as in Boldyrev and Perez (2012), the filling factor should scale as $k_\perp^{-1} \sim l_\perp$. The filling factor may be approximately estimated from the inverse scaling of the excess kurtosis (Matthaeus et al. (2015); see Sec. 4.2). Our results shown in Fig. 2(c) are indeed roughly consistent with an excess kurtosis scaling $\sim \ell_\perp^{-1}$, although this approximate scaling is overall better satisfied for δB_\parallel and δn than for δB_\perp . Finally, we mention that an alternative anisotropy estimate, based on a spectral band-pass filter (Cho and Lazarian, 2009), gives a somewhat stronger anisotropy than the five-point structure functions (not shown). On the other hand, qualitatively

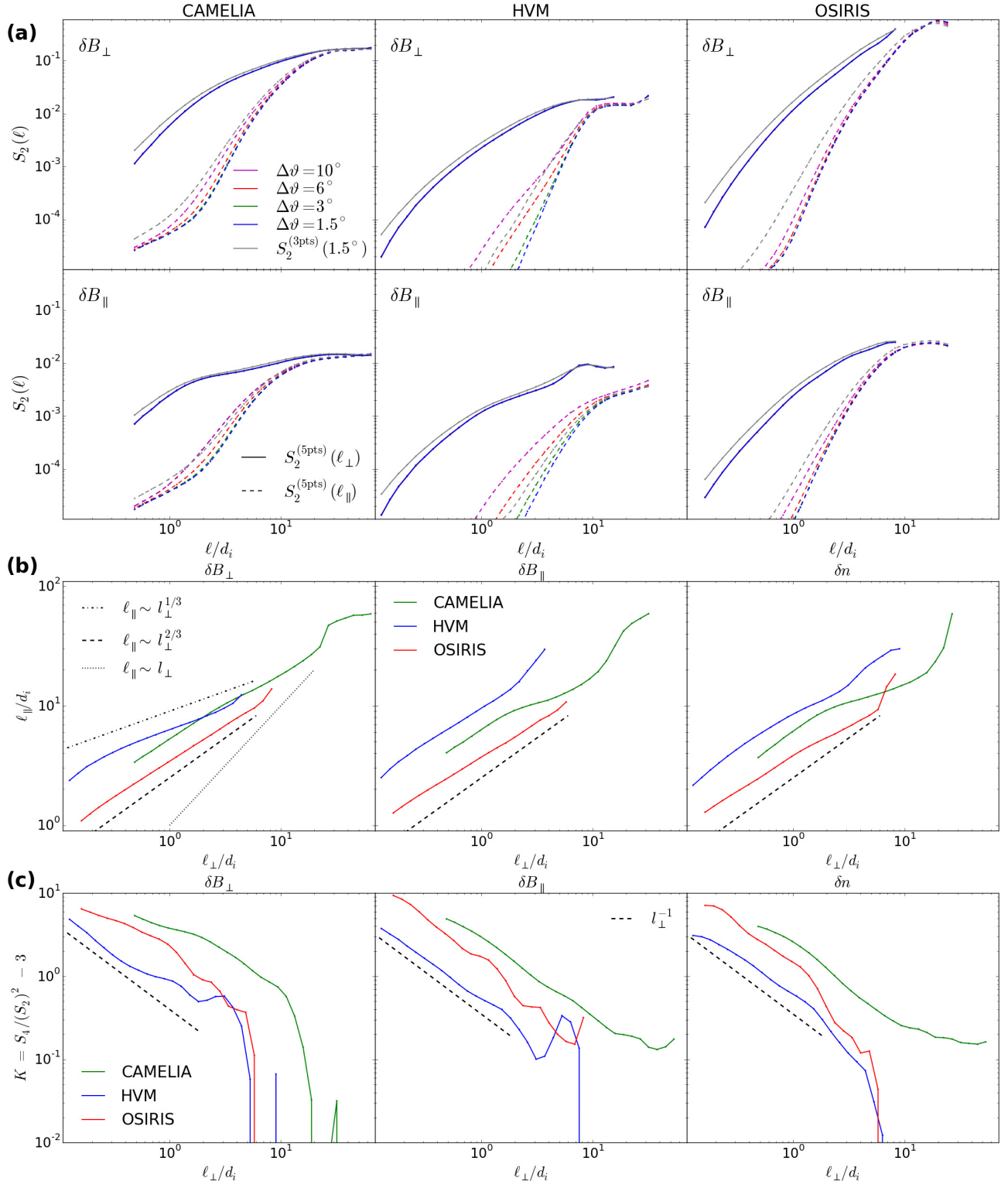


Figure 2. (a) Five-points, 2nd-order structure functions, $S_2^{(5)}$, of δB_\perp (top row) and δB_\parallel (bottom row) versus ℓ_\perp (continuous lines) and ℓ_\parallel (dashed lines). Here, \parallel and \perp are defined with respect to the local field direction (i.e., $\delta B_\parallel \neq \delta B_z$) with different angular tolerance, $\Delta\vartheta$ (colored lines; see text for definition). $S_2^{(3)}$ with $\Delta\vartheta = 1.5^\circ$ are also shown for reference (grey lines). (b) Anisotropy scaling, $\ell_\parallel(\ell_\perp)$, of δB_\perp (left panel), δB_\parallel (central panel), and δn (right panel), derived from $S_2^{(5)}$ with $\Delta\vartheta_\perp = 1.5^\circ$ nominal resolution. Three reference scalings are also shown. (c) Excess kurtosis, $K = S_4/[S_2]^2 - 3$ versus ℓ_\perp for δB_\perp (left panel), δB_\parallel (central panel), and δn (right panel). A $1/\ell_\perp$ scaling is given for reference.

similar results are still obtained for all data. Thus, all simulations analyzed exhibit a similar sub-ion-scale anisotropy according to the particular diagnostics employed. Therefore, the differences that were previously reported in the literature could be mainly related to the different methods employed.

4.2 Intermittency: the “saturation problem”

Another relevant feature of kinetic plasma turbulence is the excess kurtosis of the fluctuations, $K(\ell_{\perp}) = S_4(\ell)/[S_2(\ell)]^2 - 3$. The increase of $K(\ell_{\perp})$ above zero is a measure of non-Gaussian statistics of the turbulent fluctuations (Frisch, 1995; Matthaeus et al., 2015). As seen in Fig. 2(c), the excess kurtosis gradually increases above the Gaussian value throughout the sub-ion scale range. Moreover, similar statistical trends are seen for δB_{\perp} , δB_{\parallel} , and δn [note that we take here the component of $\delta \mathbf{B}_{\perp}$ parallel to $\ell \times \mathbf{B}_{\text{loc}}$ to estimate the flatness of δB_{\perp} (see also Kiyani et al., 2013)]. In apparent contrast with our results, a number of observational studies of solar wind turbulence find non-Gaussian, yet nearly *scale-independent* turbulence statistics at sub-ion scales (Kiyani et al., 2009; Wu et al., 2013; Kiyani et al., 2013; Chen et al., 2014). Thus, it appears a process operates in the solar wind that saturates the turbulence statistics already near the transition to sub-ion scales ($\ell_{\perp} \lesssim d_i$). What could be the reason for this apparent contradiction? One clear difference is that the solar-wind fluctuations are already heavily non-Gaussian at MHD scales (Salem et al., 2009), whereas our 3D kinetic simulations do not quite share the same feature due to the limited simulation domain. We mention that even large-size 2D kinetic simulations (e.g., Wan et al., 2012; Franci et al., 2015; Leonardis et al., 2016) did not yet achieve $K(\ell_{\perp}) \gg 1$ in the MHD range ($\ell_{\perp} \gg d_i$). In this context, it may be worth pointing out that intermittency in MHD turbulence is commonly associated with the emergence of sheetlike structures (e.g., Matthaeus et al., 2015; Chandran et al., 2015; Mallet and Schekochihin, 2017), which may break apart via the tearing instability (causing the field lines to reconnect), once their perpendicular aspect ratio exceeds a critical threshold (Matthaeus and Lamkin, 1986; Mallet et al., 2017b; Boldyrev and Loureiro, 2017). For sub-ion-scale turbulence, the possible role of magnetic reconnection has been as well highlighted in a number of recent works (e.g., Franci et al., 2016; Cerri and Califano, 2017; Franci et al., 2017; Loureiro and Boldyrev, 2017; Mallet et al., 2017a; Papini et al., 2019). Moreover, a recent observational study (Vech et al., 2018) argued that the spectral break at the tail of the MHD cascade may be controlled by reconnection. Therefore, the phenomenology of the cascade may critically depend on the morphology of the intermittent structures at the transition into the kinetic range (Mallet et al., 2017a). If the structures are indeed sufficiently sheetlike to be tearing unstable, collisionless reconnection might be one possible process that limits the growth of the sub-ion scale kurtosis (see also Biskamp et al., 1990; Chen et al., 2014). However, alternative possibilities such as collisionless damping of the fluctuations cannot be ruled out at this stage.

5 CONCLUDING REMARKS

So, what is the nature of sub-ion-scale fluctuations? From our independently performed 3D3V (hybrid and fully) kinetic simulations, a picture consistent with KAW turbulence phenomenology emerges. Moreover, our results imply a scale-dependent anisotropy, together with intermittent statistics of magnetic and density fluctuations at sub-ion scales. Thus, we conclude that within the range of parameters explored here, the statistical properties of ion-scale plasma turbulence (at $\beta \sim 1$) definitely show a certain degree of similarity, regardless of the precise details of the large-scale energy injection. On the other hand, slight differences can also be identified, some of which may be also model-dependent.

A number of key aspects will have to await the next-generation of 3D3V kinetic simulations. Ideally, future numerical experiments should aim to resolve both larger (MHD) scales, as well as a broader range

between the ion and the electron scales by adopting significantly higher (if not realistic) mass ratios. These two aspects indeed appear to be both required in order to achieve (i) a possible saturation of the kurtosis at ion scales and (ii) a relevant sub-ion range of scales before electron-scale effects significantly come into play. Moreover, different aspects other than the spectral and statistical properties of the turbulent fluctuations will need to be considered in characterizing kinetic-range turbulence, as for instance, the dissipation mechanisms of turbulent fluctuations under different plasma conditions and the consequent energy partition among different species (e.g., Matthaeus et al., 2016; Parashar et al., 2018; Arzamasskiy et al., 2019; Kawazura et al., 2019; Zhdankin et al., 2019).

While certain progress was definitely achieved in recent years, many other plasma regimes and setups may need to be explored, and the process(es) underlying a possible universality of kinetic-range plasma turbulence (e.g., magnetic reconnection) need to be fully worked out. Moreover, a few relevant discrepancies between numerical simulations, theories and *in-situ* observations appear. These “anomalies” definitely call for an explanation by the space physics community. In this context, advances cannot be achieved without investing in next-generation *multi-spacecraft* missions. Multi-point *in situ* measurements of turbulent fluctuations from a large number of spacecrafts are indeed fundamental in order to disentangle the nonlinear spatio-temporal character of plasma turbulence (see, e.g., Klein et al., 2019; Matthaeus et al., 2019; TenBarge et al., 2019). This includes answering fundamental questions about, for instance, (i) the distribution of turbulent energy in space and time, (ii) the three-dimensional anisotropic structure of energy transfer across scales, (iii) the high-order statistics of the fluctuations, and (iv) the validity of Taylor’s hypothesis over a broad range of time and spatial scales. Alongside observations, advances in computational capabilities are required to perform more realistic numerical simulations as discussed above, and compare these with spacecraft measurements. Finally, following the same spirit promoted by the “Turbulent Dissipation Challenge” (Parashar et al., 2015), we would like to end this Perspective by stressing that our community could benefit from comparisons such as the one performed here, involving various codes, models and diagnostics.

Note added: Arzamasskiy et al. (2019) recently reported a scale-independent anisotropy at ion scales (i.e., $\ell_{\parallel} \sim \ell_{\perp}$) based on a set of 3D driven hybrid-kinetic turbulence simulations. Using our structure function diagnostic applied to their data, we were able to qualitatively (and quantitatively) reproduce their result. A more detailed investigation along these lines is currently ongoing, but beyond the scope of this Perspective and will be presented elsewhere.

CONFLICT OF INTEREST STATEMENT

The authors declare that the research was conducted in the absence of any commercial or financial relationships that could be construed as a potential conflict of interest.

AUTHOR CONTRIBUTIONS

SSC, DG, and LF provided their HVM, OSIRIS and CAMELIA simulation data, respectively. SSC performed the spectral analysis, produced the figures, and wrote the paper, taking into account suggestions from DG and LF. DG implemented and performed the structure function analysis. All authors discussed the results.

FUNDING

SSC is supported by the National Aeronautics and Space Administration under Grant No. NNX16AK09G issued through the Heliophysics Supporting Research Program. LF is supported by the UK Science and Technology Facilities Council (STFC) grant ST/P000622/1.

ACKNOWLEDGMENTS

SSC and DG acknowledge the generous hospitality of the Wolfgang Pauli Institute in Vienna, where the first discussions leading to this work took place. We acknowledge PRACE for awarding us access to Marconi at CINECA, Italy, where the calculations with the HVM code were performed under the grant No. 2017174107. The Cray XC40, Shaheen, at the King Abdullah University of Science & Technology (KAUST) in Thuwal, Saudi Arabia was utilized for the simulation performed with the OSIRIS code. LF acknowledges PRACE for awarding him access to Cartesius at SURFsara, the Netherlands, through the DECI-13 (Distributed European Computing Initiative) call (project HybTurb3D) where the HPIC simulation was performed, and INAF and CINECA for awarding him access to Marconi within the framework of the MoU “New Frontiers in Astrophysics: HPC and New Generation Data Exploration” (project INA17_C4A26), where new further analysis of the HPIC data has been performed. The authors would like to acknowledge the OSIRIS Consortium, consisting of UCLA and IST (Lisbon, Portugal) for the use of OSIRIS 3.0 and for providing access to the OSIRIS 3.0 framework. SSC acknowledges Dr. C. Cavazzoni and Dr. M. Guarrasi (CINECA, Italy) for their contributions to HVM code parallelization, performance and implementation on Marconi-KNL. The authors also acknowledge useful discussions with Alfred Mallet, Lev Arzamasskiy, Bill Dorland, Matt Kunz, Simone Landi, Emanuele Papini, Frank Jenko, and David Burgess.

DATA AVAILABILITY STATEMENT

The data used in this study are available from the authors upon reasonable request.

REFERENCES

- Adkins, T. and Schekochihin, A. A. (2018). A solvable model of Vlasov-kinetic plasma turbulence in Fourier-Hermite phase space. *J. Plasma Phys.* 84, 905840107. doi:10.1017/S0022377818000089
- Alexandrova, O., Chen, C. H. K., Sorriso-Valvo, L., Horbury, T. S., and Bale, S. D. (2013). Solar Wind Turbulence and the Role of Ion Instabilities. *Space Sci. Rev.* 178, 101–139. doi:10.1007/s11214-013-0004-8
- Alexandrova, O., Lacombe, C., Mangeney, A., Grappin, R., and Maksimovic, M. (2012). Solar Wind Turbulent Spectrum at Plasma Kinetic Scales. *Astrophys. J.* 760, 121. doi:10.1088/0004-637X/760/2/121
- Alexandrova, O., Saur, J., Lacombe, C., Mangeney, A., Mitchell, J., Schwartz, S. J., et al. (2009). Universality of Solar-Wind Turbulent Spectrum from MHD to Electron Scales. *Phys. Rev. Lett.* 103, 165003. doi:10.1103/PhysRevLett.103.165003
- Arzamasskiy, L., Kunz, M. W., Chandran, B. D. G., and Quataert, E. (2019). Hybrid-kinetic Simulations of Ion Heating in Alfvénic Turbulence. *Astrophys. J.* 879, 53. doi:10.3847/1538-4357/ab20cc
- Bañón Navarro, A., Teaca, B., Told, D., Groselj, D., Crandall, P., and Jenko, F. (2016). Structure of Plasma Heating in Gyrokinetic Alfvénic Turbulence. *Phys. Rev. Lett.* 117, 245101. doi:10.1103/PhysRevLett.117.245101
- Biskamp, D. (2008). *Magnetohydrodynamic Turbulence* (Cambridge University Press, Cambridge, UK)

- Biskamp, D., Welter, H., and Walter, M. (1990). Statistical Properties of Two-Dimensional Magnetohydrodynamic Turbulence. *Phys. Fluids B* 2, 3024. doi:10.1063/1.859369
- Boldyrev, S., Horaites, K., Xia, Q., and Perez, J. C. (2013). Toward a Theory of Astrophysical Plasma Turbulence at Subproton Scales. *Astrophys. J.* 777, 41. doi:10.1088/0004-637X/777/1/41
- Boldyrev, S. and Loureiro, N. F. (2017). Magnetohydrodynamic Turbulence Mediated by Reconnection. *Astrophys. J.* 844, 125. doi:10.3847/1538-4357/aa7d02
- Boldyrev, S. and Perez, J. C. (2012). Spectrum of Kinetic-Alfvén Turbulence. *Astrophys. J. Lett.* 758, L44. doi:10.1088/2041-8205/758/2/L44
- Bruno, R. and Carbone, V. (2013). The Solar Wind as a Turbulence Laboratory. *Living Rev. Sol. Phys.* 10. doi:10.12942/lrsp-2013-2
- Cerri, S. S. and Califano, F. (2017). Reconnection and small-scale fields in 2D-3V hybrid-kinetic driven turbulence simulations. *New J. Phys.* 19, 025007. doi:10.1088/1367-2630/aa5c4a
- Cerri, S. S., Califano, F., Jenko, F., Told, D., and Rincon, F. (2016). Subproton-scale Cascades in Solar Wind Turbulence: Driven Hybrid-kinetic Simulations. *Astrophys. J. Lett.* 822, L12. doi:10.3847/2041-8205/822/1/L12
- Cerri, S. S., Franci, L., Califano, F., Landi, S., and Hellinger, P. (2017a). Plasma turbulence at ion scales: a comparison between particle in cell and Eulerian hybrid-kinetic approaches. *J. Plasma Phys.* 83, 705830202. doi:10.1017/S0022377817000265
- Cerri, S. S., Kunz, M. W., and Califano, F. (2018). Dual Phase-space Cascades in 3D Hybrid-Vlasov-Maxwell Turbulence. *Astrophys. J. Lett.* 856, L13. doi:10.3847/2041-8213/aab557
- Cerri, S. S., Servidio, S., and Califano, F. (2017b). Kinetic Cascade in Solar-wind Turbulence: 3D3V Hybrid-kinetic Simulations with Electron Inertia. *Astrophys. J. Lett.* 846, L18. doi:10.3847/2041-8213/aa87b0
- Chandran, B. D. G., Schekochihin, A. A., and Mallet, A. (2015). Intermittency and Alignment in Strong RMHD Turbulence. *Astrophys. J.* 807, 39. doi:10.1088/0004-637X/807/1/39
- Chasapis, A., Matthaeus, W. H., Parashar, T. N., Fuselier, S. A., Maruca, B. A., Phan, T. D., et al. (2017). High-resolution Statistics of Solar Wind Turbulence at Kinetic Scales Using the Magnetospheric Multiscale Mission. *Astrophys. J. Lett.* 844, L9. doi:10.3847/2041-8213/aa7ddd
- Chen, C. H. K. (2016). Recent progress in astrophysical plasma turbulence from solar wind observations. *J. Plasma Phys.* 82, 535820602. doi:10.1017/S0022377816001124
- Chen, C. H. K. and Boldyrev, S. (2017). Nature of Kinetic Scale Turbulence in the Earth's Magnetosheath. *Astrophys. J.* 842, 122. doi:10.3847/1538-4357/aa74e0
- Chen, C. H. K., Boldyrev, S., Xia, Q., and Perez, J. C. (2013). Nature of Subproton Scale Turbulence in the Solar Wind. *Phys. Rev. Lett.* 110, 225002. doi:10.1103/PhysRevLett.110.225002
- Chen, C. H. K., Horbury, T. S., Schekochihin, A. A., Wicks, R. T., Alexandrova, O., and Mitchell, J. (2010). Anisotropy of Solar Wind Turbulence between Ion and Electron Scales. *Phys. Rev. Lett.* 104, 255002. doi:10.1103/PhysRevLett.104.255002
- Chen, C. H. K., Klein, K. G., and Howes, G. G. (2019). Evidence for electron Landau damping in space plasma turbulence. *Nature Communications* 10, 740. doi:10.1038/s41467-019-08435-3
- Chen, C. H. K., Sorriso-Valvo, L., Šafránková, J., and Němeček, Z. (2014). Intermittency of Solar Wind Density Fluctuations from Ion to Electron Scales. *Astrophys. J. Lett.* 789, L8. doi:10.1088/2041-8205/789/1/L8
- Cho, J. (2019). A Technique for Removing Large-scale Variations in Regularly and Irregularly Spaced Data. *Astrophys. J.* 874, 75. doi:10.3847/1538-4357/ab06f3

- Cho, J. and Lazarian, A. (2004). The Anisotropy of Electron Magnetohydrodynamic Turbulence. *Astrophys. J. Lett.* 615, L41–L44. doi:10.1086/425215
- Cho, J. and Lazarian, A. (2009). Simulations of Electron Magnetohydrodynamic Turbulence. *Astrophys. J.* 701, 236–252. doi:10.1088/0004-637X/701/1/236
- Cho, J. and Vishniac, E. T. (2000). The Anisotropy of Magnetohydrodynamic Alfvénic Turbulence. *Astrophys. J.* 539, 273–282. doi:10.1086/309213
- Comişel, H., Nariyuki, Y., Narita, Y., and Motschmann, U. (2016). On the role of ion-scale whistler waves in space and astrophysical plasma turbulence. *Annales Geophysicae* 34, 975–984. doi:10.5194/angeo-34-975-2016
- Del Sarto, D., Pegoraro, F., and Tenerani, A. (2017). ‘Magneto-elastic’ waves in an anisotropic magnetised plasma. *Plasma Phys. Control. Fusion* 59, 045002. doi:10.1088/1361-6587/aa56bd
- Eyink, G. L. (2018). Cascades and Dissipative Anomalies in Nearly Collisionless Plasma Turbulence. *Physical Review X* 8, 041020. doi:10.1103/PhysRevX.8.041020
- Falcon, E., Fauve, S., and Laroche, C. (2007). Observation of intermittency in wave turbulence. *Phys. Rev. Lett.* 98, 154501. doi:10.1103/PhysRevLett.98.154501
- Fonseca, R. A., Silva, L. O., Tsung, F. S., Decyk, V. K., Lu, W., Ren, C., et al. (2002). OSIRIS: A Three-Dimensional, Fully Relativistic Particle in Cell Code for Modeling Plasma Based Accelerators. *Lecture Notes in Comput. Sci.* 2331, 342. doi:10.1007/3-540-47789-6_36
- Fonseca, R. A., Vieira, J., Fiuza, F., Davidson, A., Tsung, F. S., Mori, W. B., et al. (2013). Exploiting Multi-Scale Parallelism for Large Scale Numerical Modelling of Laser Wakefield Accelerators. *Plasma Phys. Control. Fusion* 55, 124011. doi:10.1088/0741-3335/55/12/124011
- Franci, L., Cerri, S. S., Califano, F., Landi, S., Papini, E., Verdini, A., et al. (2017). Magnetic Reconnection as a Driver for a Sub-ion-scale Cascade in Plasma Turbulence. *Astrophys. J. Lett.* 850, L16. doi:10.3847/2041-8213/aa93fb
- Franci, L., Hellinger, P., Guarrasi, M., Chen, C. H. K., Papini, E., Verdini, A., et al. (2018a). Three-dimensional simulations of solar wind turbulence with the hybrid code camelia. *J. Phys. Conf. Ser.* 1031, 012002. doi:10.1088/1742-6596/1031/1/012002
- Franci, L., Landi, S., Matteini, L., Verdini, A., and Hellinger, P. (2015). High-resolution Hybrid Simulations of Kinetic Plasma Turbulence at Proton Scales. *Astrophys. J.* 812, 21. doi:10.1088/0004-637X/812/1/21
- Franci, L., Landi, S., Matteini, L., Verdini, A., and Hellinger, P. (2016). Plasma Beta Dependence of the Ion-scale Spectral Break of Solar Wind Turbulence: High-resolution 2D Hybrid Simulations. *Astrophys. J.* 833, 91. doi:10.3847/1538-4357/833/1/91
- Franci, L., Landi, S., Verdini, A., Matteini, L., and Hellinger, P. (2018b). Solar Wind Turbulent Cascade from MHD to Sub-ion Scales: Large-size 3D Hybrid Particle-in-cell Simulations. *Astrophys. J.* 853, 26. doi:10.3847/1538-4357/aaa3e8
- Frisch, U. (1995). *Turbulence. The legacy of A. N. Kolmogorov* (Cambridge University Press, Cambridge, UK)
- Galtier, S. and Bhattacharjee, A. (2003). Anisotropic weak whistler wave turbulence in electron magnetohydrodynamics. *Phys. Plasmas* 10, 3065–3076. doi:10.1063/1.1584433
- Gary, S. P., Chang, O., and Wang, J. (2012). Forward Cascade of Whistler Turbulence: Three-dimensional Particle-in-cell Simulations. *Astrophys. J.* 755, 142. doi:10.1088/0004-637X/755/2/142
- Gary, S. P. and Nishimura, K. (2004). Kinetic Alfvén waves: Linear theory and a particle-in-cell simulation. *J. Geophys. Res.* 109, A02109. doi:10.1029/2003JA010239
- Gary, S. P. and Smith, C. W. (2009). Short-wavelength turbulence in the solar wind: Linear theory of whistler and kinetic Alfvén fluctuations. *J. Geophys. Res.* 114, A12105. doi:10.1029/2009JA014525

- Greco, A., Perri, S., Servidio, S., Yordanova, E., and Veltri, P. (2016). The Complex Structure of Magnetic Field Discontinuities in the Turbulent Solar Wind. *Astrophys. J.* 823, L39. doi:10.3847/2041-8205/823/2/L39
- Grošelj, D., Cerri, S. S., Bañón Navarro, A., Willmott, C., Told, D., Loureiro, N. F., et al. (2017). Fully Kinetic versus Reduced-kinetic Modeling of Collisionless Plasma Turbulence. *Astrophys. J.* 847, 28. doi:10.3847/1538-4357/aa894d
- Grošelj, D., Chen, C. H. K., Mallet, A., Samtaney, R., Schneider, K., and Jenko, F. (2019). Kinetic Turbulence in Astrophysical Plasmas: Waves and/or Structures? *Physical Review X* 9, 031037. doi:10.1103/PhysRevX.9.031037
- Grošelj, D., Mallet, A., Loureiro, N. F., and Jenko, F. (2018). Fully Kinetic Simulation of 3D Kinetic Alfvén Turbulence. *Phys. Rev. Lett.* 120, 105101. doi:10.1103/PhysRevLett.120.105101
- He, J., Tu, C., Marsch, E., and Yao, S. (2012). Do Oblique Alfvén/Ion-cyclotron or Fast-mode/Whistler Waves Dominate the Dissipation of Solar Wind Turbulence near the Proton Inertial Length? *Astrophys. J. Lett.* 745, L8. doi:10.1088/2041-8205/745/1/L8
- Hollweg, J. V. (1999). Kinetic Alfvén wave revisited. *J. Geophys. Res.* 104, 14811–14820. doi:10.1029/1998JA900132
- Howes, G. G., Cowley, S. C., Dorland, W., Hammett, G. W., Quataert, E., and Schekochihin, A. A. (2008a). A model of turbulence in magnetized plasmas: Implications for the dissipation range in the solar wind. *J. Geophys. Res.* 113, A05103. doi:10.1029/2007JA012665
- Howes, G. G., Dorland, W., Cowley, S. C., Hammett, G. W., Quataert, E., Schekochihin, A. A., et al. (2008b). Kinetic Simulations of Magnetized Turbulence in Astrophysical Plasmas. *Phys. Rev. Lett.* 100, 065004. doi:10.1103/PhysRevLett.100.065004
- Howes, G. G., Tenbarge, J. M., and Dorland, W. (2011). A weakened cascade model for turbulence in astrophysical plasmas. *Phys. Plasmas* 18, 102305–102305. doi:10.1063/1.3646400
- Huang, S. Y., Hadid, L. Z., Sahraoui, F., Yuan, Z. G., and Deng, X. H. (2017). On the Existence of the Kolmogorov Inertial Range in the Terrestrial Magnetosheath Turbulence. *Astrophys. J. Lett.* 836, L10. doi:10.3847/2041-8213/836/1/L10
- Hughes, R. S., Gary, S. P., and Wang, J. (2017a). Particle-in-cell Simulations of Electron and Ion Dissipation by Whistler Turbulence: Variations with Electron β . *Astrophys. J.* 835, L15. doi:10.3847/2041-8213/835/1/L15
- Hughes, R. S., Gary, S. P., Wang, J., and Parashar, T. N. (2017b). Kinetic Alfvén Turbulence: Electron and Ion Heating by Particle-in-cell Simulations. *Astrophys. J. Lett.* 847, L14. doi:10.3847/2041-8213/aa8b13
- Kawazura, Y., Barnes, M., and Schekochihin, A. A. (2019). Thermal disequilibrium of ions and electrons by collisionless plasma turbulence. *Proceedings of the National Academy of Sciences* 116, 771–776. doi:10.1073/pnas.1812491116
- Kiyani, K. H., Chapman, S. C., Khotyaintsev, Y. V., Dunlop, M. W., and Sahraoui, F. (2009). Global Scale-Invariant Dissipation in Collisionless Plasma Turbulence. *Phys. Rev. Lett.* 103, 075006. doi:10.1103/PhysRevLett.103.075006
- Kiyani, K. H., Chapman, S. C., Sahraoui, F., Hnat, B., Fauvarque, O., and Khotyaintsev, Y. V. (2013). Enhanced Magnetic Compressibility and Isotropic Scale Invariance at Sub-ion Larmor Scales in Solar Wind Turbulence. *Astrophys. J.* 763, 10. doi:10.1088/0004-637X/763/1/10
- Klein, K. G., Alexandrova, O., Bookbinder, J., Caprioli, D., Case, A. W., Chandran, B. D. G., et al. (2019). [Plasma 2020 Decadal] Multipoint Measurements of the Solar Wind: A Proposed Advance for Studying Magnetized Turbulence. *arXiv e-prints*, arXiv:1903.05740

- Kobayashi, S., Sahraoui, F., Passot, T., Laveder, D., Sulem, P. L., Huang, S. Y., et al. (2017). Three-dimensional Simulations and Spacecraft Observations of Sub-ion Scale Turbulence in the Solar Wind: Influence of Landau Damping. *Astrophys. J.* 839, 122. doi:10.3847/1538-4357/aa67f2
- Kunz, M. W., Abel, I. G., Klein, K. G., and Schekochihin, A. A. (2018). Astrophysical gyrokinetics: turbulence in pressure-anisotropic plasmas at ion scales and beyond. *J. Plasma Phys.* 84, 715840201. doi:10.1017/S0022377818000296
- Lacombe, C., Alexandrova, O., and Matteini, L. (2017). Anisotropies of the Magnetic Field Fluctuations at Kinetic Scales in the Solar Wind: Cluster Observations. *Astrophys. J.* 848, 45. doi:10.3847/1538-4357/aa8c06
- Landi, S., Franci, L., Papini, E., Verdini, A., Matteini, L., and Hellinger, P. (2019). Spectral anisotropies and intermittency of plasma turbulence at ion kinetic scales. *arXiv e-prints*, arXiv:1904.03903
- Leamon, R. J., Smith, C. W., Ness, N. F., Matthaeus, W. H., and Wong, H. K. (1998). Observational constraints on the dynamics of the interplanetary magnetic field dissipation range. *J. Geophys. Res.* 103, 4775–4788. doi:10.1029/97JA03394
- Leonardis, E., Sorriso-Valvo, L., Valentini, F., Servidio, S., Carbone, F., and Veltri, P. (2016). Multifractal scaling and intermittency in hybrid Vlasov-Maxwell simulations of plasma turbulence. *Phys. Plasmas* 23, 022307. doi:10.1063/1.4942417
- Loureiro, N. L. and Boldyrev, S. (2017). Collisionless reconnection in magnetohydrodynamic and kinetic turbulence. *Astrophys. J.* 850, 182
- Mallet, A. and Schekochihin, A. A. (2017). A Statistical Model of Three-Dimensional Anisotropy and Intermittency in Strong Alfvénic Turbulence. *Mon. Not. R. Astron. Soc.* 466, 3918. doi:10.1093/mnras/stw3251
- Mallet, A., Schekochihin, A. A., and Chandran, B. D. G. (2017a). Disruption of Alfvénic turbulence by magnetic reconnection in a collisionless plasma. *J. Plasma Phys.* 83. doi:10.1017/S0022377817000812
- Mallet, A., Schekochihin, A. A., and Chandran, B. D. G. (2017b). Disruption of sheet-like structures in Alfvénic turbulence by magnetic reconnection. *Mon. Not. R. Astron. Soc.* 468, 4862–4871. doi:10.1093/mnras/stx670
- Mallet, A., Schekochihin, A. A., Chandran, B. D. G., Chen, C. H. K., Horbury, T. S., Wicks, R. T., et al. (2016). Measures of Three-Dimensional Anisotropy and Intermittency in Strong Alfvénic Turbulence. *Mon. Not. R. Astron. Soc.* 459, 2130. doi:10.1093/mnras/stw802
- Matthaeus, W. H., Bandyopadhyay, R., Brown, M. R., Borovsky, J., Carbone, V., Caprioli, D., et al. (2019). [Plasma 2020 Decadal] The essential role of multi-point measurements in turbulence investigations: the solar wind beyond single scale and beyond the Taylor Hypothesis. *arXiv e-prints*, arXiv:1903.06890
- Matthaeus, W. H. and Lamkin, S. L. (1986). Turbulent magnetic reconnection. *Phys. Fluids* 29, 2513–2534. doi:10.1063/1.866004
- Matthaeus, W. H., Oughton, S., Osman, K. T., Servidio, S., Wan, M., Gary, S. P., et al. (2014). Nonlinear and Linear Timescales near Kinetic Scales in Solar Wind Turbulence. *Astrophys. J.* 790, 155. doi:10.1088/0004-637X/790/2/155
- Matthaeus, W. H., Parashar, T. N., Wan, M., and Wu, P. (2016). Turbulence and Proton-Electron Heating in Kinetic Plasma. *Astrophys. J. Lett.* 827, L7. doi:10.3847/2041-8205/827/1/L7
- Matthaeus, W. H., Wan, M., Servidio, S., Greco, A., Osman, K. T., Oughton, S., et al. (2015). Intermittency, nonlinear dynamics and dissipation in the solar wind and astrophysical plasmas. *Philosophical Transactions of the Royal Society of London Series A* 373, 20140154–20140154. doi:10.1098/rsta.2014.0154

- Meyrand, R., Kanekar, A., Dorland, W., and Schekochihin, A. A. (2019). Fluidization of collisionless plasma turbulence. *Proceedings of the National Academy of Science* 116, 1185–1194. doi:10.1073/pnas.1813913116
- Narita, Y., Nakamura, R., Baumjohann, W., Glassmeier, K.-H., Motschmann, U., Giles, B., et al. (2016). On Electron-scale Whistler Turbulence in the Solar Wind. *Astrophys. J. Lett.* 827, L8. doi:10.3847/2041-8205/827/1/L8
- Omidi, N., Isenberg, P., Russell, C. T., Jian, L. K., and Wei, H. Y. (2014). Generation of ion cyclotron waves in the corona and solar wind. *J. Geophys. Res.* 119, 1442–1454. doi:10.1002/2013JA019474
- Papini, E., Franci, L., Landi, S., Verdini, A., Matteini, L., and Hellinger, P. (2019). Can Hall Magnetohydrodynamics Explain Plasma Turbulence at Sub-ion Scales? *Astrophys. J.* 870, 52. doi:10.3847/1538-4357/aaf003
- Parashar, T. N., Matthaeus, W. H., and Shay, M. A. (2018). Dependence of Kinetic Plasma Turbulence on Plasma β . *Astrophys. J. Lett.* 864, L21. doi:10.3847/2041-8213/aadb8b
- Parashar, T. N., Salem, C., Wicks, R. T., Karimabadi, H., Gary, S. P., and Matthaeus, W. H. (2015). Turbulent dissipation challenge: a community-driven effort. *J. Plasma Phys.* 81, 905810513. doi:10.1017/S0022377815000860
- Passot, T. and Sulem, P. L. (2015). A Model for the Non-universal Power Law of the Solar Wind Sub-ion-scale Magnetic Spectrum. *Astrophys. J. Lett.* 812, L37. doi:10.1088/2041-8205/812/2/L37
- Passot, T. and Sulem, P. L. (2019). Imbalanced kinetic Alfvén wave turbulence: from weak turbulence theory to nonlinear diffusion models for the strong regime. *arXiv e-prints*, arXiv:1902.04295
- Passot, T., Sulem, P. L., and Tassi, E. (2018). Gyrofluid modeling and phenomenology of low- β_e Alfvén wave turbulence. *Phys. Plasmas* 25, 042107. doi:10.1063/1.5022528
- Pezzi, O., Servidio, S., Perrone, D., Valentini, F., Sorriso-Valvo, L., Greco, A., et al. (2018). Velocity-space cascade in magnetized plasmas: Numerical simulations. *Phys. Plasmas* 25, 060704. doi:10.1063/1.5027685
- Podesta, J. J. (2012). The need to consider ion Bernstein waves as a dissipation channel of solar wind turbulence. *J. Geophys. Res.* 117, A07101. doi:10.1029/2012JA017770
- Podesta, J. J. and TenBarge, J. M. (2012). Scale dependence of the variance anisotropy near the proton gyroradius scale: Additional evidence for kinetic Alfvén waves in the solar wind at 1 AU. *J. Geophys. Res.* 117, A10106. doi:10.1029/2012JA017724
- Pucci, F., Váscónez, C. L., Pezzi, O., Servidio, S., Valentini, F., Matthaeus, W. H., et al. (2016). From Alfvén waves to kinetic Alfvén waves in an inhomogeneous equilibrium structure. *J. Geophys. Res.* 121, 1024–1045. doi:10.1002/2015JA022216
- Roberts, O. W., Narita, Y., and Escoubet, C. P. (2017). Direct Measurement of Anisotropic and Asymmetric Wave Vector Spectrum in Ion-scale Solar Wind Turbulence. *Astrophys. J.* 851, L11. doi:10.3847/2041-8213/aa9bf3
- Roytershteyn, V., Boldyrev, S., Delzanno, G. L., Chen, C. H. K., Grošelj, D., and Loureiro, N. F. (2019). Numerical Study of Inertial Kinetic-Alfvén Turbulence. *Astrophys. J.* 870, 103. doi:10.3847/1538-4357/aaf288
- Sahraoui, F., Belmont, G., and Goldstein, M. L. (2012). New Insight into Short-wavelength Solar Wind Fluctuations from Vlasov Theory. *Astrophys. J.* 748, 100. doi:10.1088/0004-637X/748/2/100
- Sahraoui, F., Goldstein, M. L., Belmont, G., Canu, P., and Rezeau, L. (2010). Three Dimensional Anisotropic k Spectra of Turbulence at Subproton Scales in the Solar Wind. *Phys. Rev. Lett.* 105, 131101. doi:10.1103/PhysRevLett.105.131101

- Sahraoui, F., Goldstein, M. L., Robert, P., and Khotyaintsev, Y. V. (2009). Evidence of a Cascade and Dissipation of Solar-Wind Turbulence at the Electron Gyroscale. *Phys. Rev. Lett.* 102, 231102. doi:10.1103/PhysRevLett.102.231102
- Salem, C., Mangeney, A., Bale, S. D., and Veltri, P. (2009). Solar Wind Magnetohydrodynamics Turbulence: Anomalous Scaling and Role of Intermittency. *Astrophys. J.* 702, 537. doi:10.1088/0004-637X/702/1/537
- Salem, C. S., Howes, G. G., Sundkvist, D., Bale, S. D., Chaston, C. C., Chen, C. H. K., et al. (2012). Identification of Kinetic Alfvén Wave Turbulence in the Solar Wind. *Astrophys. J. Lett.* 745, L9. doi:10.1088/2041-8205/745/1/L9
- Schekochihin, A. A., Cowley, S. C., Dorland, W., Hammett, G. W., Howes, G. G., Plunk, G. G., et al. (2008). Gyrokinetic turbulence: a nonlinear route to dissipation through phase space. *Plasma Physics and Controlled Fusion* 50, 124024. doi:10.1088/0741-3335/50/12/124024
- Schekochihin, A. A., Cowley, S. C., Dorland, W., Hammett, G. W., Howes, G. G., Quataert, E., et al. (2009). Astrophysical Gyrokinetics: Kinetic and Fluid Turbulent Cascades in Magnetized Weakly Collisional Plasmas. *Astrophys. J.* 182, 310–377. doi:10.1088/0067-0049/182/1/310
- Schneider, K., Farge, M., and Kevlahan, N. (2004). Spatial intermittency in two-dimensional turbulence: A wavelet approach. In *Woods Hole Mathematics, Perspectives in Mathematics and Physics*, eds. N. Tongring and R. C. Penner (World Scientific), vol. 34. 302–328. doi:10.1142/9789812701398_0007
- Servidio, S., Chasapis, A., Matthaeus, W. H., Perrone, D., Valentini, F., Parashar, T. N., et al. (2017). Magnetospheric Multiscale Observation of Plasma Velocity-Space Cascade: Hermite Representation and Theory. *Phys. Rev. Lett.* 119, 205101. doi:10.1103/PhysRevLett.119.205101
- Servidio, S., Valentini, F., Perrone, D., Greco, A., Califano, F., Matthaeus, W. H., et al. (2015). A kinetic model of plasma turbulence. *J. Plasma Phys.* 81, 325810107. doi:10.1017/S0022377814000841
- Sorriso-Valvo, L., Carbone, F., Perri, S., Greco, A., Marino, R., and Bruno, R. (2018). On the Statistical Properties of Turbulent Energy Transfer Rate in the Inner Heliosphere. *Sol. Phys.* 293, 10. doi:10.1007/s11207-017-1229-6
- Stawicki, O., Gary, S. P., and Li, H. (2001). Solar wind magnetic fluctuation spectra: Dispersion versus damping. *J. Geophys. Res.* 106, 8273–8282. doi:10.1029/2000JA000446
- TenBarge, J. M., Alexandrova, O., Boldyrev, S., Califano, F., Cerri, S. S., Chen, C. H. K., et al. (2019). [Plasma 2020 Decadal] Disentangling the Spatiotemporal Structure of Turbulence Using Multi-Spacecraft Data. *arXiv e-prints*, arXiv:1903.05710
- TenBarge, J. M. and Howes, G. G. (2013). Current Sheets and Collisionless Damping in Kinetic Plasma Turbulence. *Astrophys. J. Lett.* 771, L27. doi:10.1088/2041-8205/771/2/L27
- TenBarge, J. M., Podesta, J. J., Klein, K. G., and Howes, G. G. (2012). Interpreting Magnetic Variance Anisotropy Measurements in the Solar Wind. *Astrophys. J.* 753, 107. doi:10.1088/0004-637X/753/2/107
- Told, D., Cookmeyer, J., Muller, F., Astfalk, P., and Jenko, F. (2016). Comparative study of gyrokinetic, hybrid-kinetic and fully kinetic wave physics for space plasmas. *New J. Phys.* 18, 065011. doi:10.1088/1367-2630/18/6/065011
- Told, D., Jenko, F., TenBarge, J. M., Howes, G. G., and Hammett, G. W. (2015). Multiscale Nature of the Dissipation Range in Gyrokinetic Simulations of Alfvénic Turbulence. *Phys. Rev. Lett.* 115, 025003. doi:10.1103/PhysRevLett.115.025003
- Valentini, F., Trávníček, P., Califano, F., Hellinger, P., and Mangeney, A. (2007). A hybrid-Vlasov model based on the current advance method for the simulation of collisionless magnetized plasma. *JCoPh* 225, 753–770. doi:10.1016/j.jcp.2007.01.001

- Valentini, F., Váscónez, C. L., Pezzi, O., Servidio, S., Malara, F., and Pucci, F. (2017). Transition to kinetic turbulence at proton scales driven by large-amplitude kinetic Alfvén fluctuations. *Astron. Astrophys.* 599, A8. doi:10.1051/0004-6361/201629240
- Váscónez, C. L., Pucci, F., Valentini, F., Servidio, S., Matthaeus, W. H., and Malara, F. (2015). Kinetic Alfvén Wave Generation by Large-scale Phase Mixing. *Astrophys. J.* 815, 7. doi:10.1088/0004-637X/815/1/7
- Váscónez, C. L., Valentini, F., Camporeale, E., and Veltri, P. (2014). Vlasov simulations of kinetic Alfvén waves at proton kinetic scales. *Phys. Plasmas* 21, 112107. doi:10.1063/1.4901583
- Vasquez, B. J., Markovskii, S. A., and Chandran, B. D. G. (2014). Three-dimensional Hybrid Simulation Study of Anisotropic Turbulence in the Proton Kinetic Regime. *Astrophys. J.* 788, 178. doi:10.1088/0004-637X/788/2/178
- Vech, D., Mallet, A., Klein, K. G., and Kasper, J. C. (2018). Magnetic Reconnection May Control the Ion-scale Spectral Break of Solar Wind Turbulence. *Astrophys. J. Lett.* 855, L27. doi:10.3847/2041-8213/aab351
- Verscharen, D., Klein, K. G., and Maruca, B. A. (2019). The multi-scale nature of the solar wind. *arXiv e-prints*, arXiv:1902.03448
- Wan, M., Matthaeus, W. H., Karimabadi, H., Roytershteyn, V., Shay, M., Wu, P., et al. (2012). Intermittent Dissipation at Kinetic Scales in Collisionless Plasma Turbulence. *Phys. Rev. Lett.* 109, 195001. doi:10.1103/PhysRevLett.109.195001
- Wan, M., Matthaeus, W. H., Roytershteyn, V., Karimabadi, H., Parashar, T., Wu, P., et al. (2015). Intermittent Dissipation and Heating in 3D Kinetic Plasma Turbulence. *Phys. Rev. Lett.* 114, 175002. doi:10.1103/PhysRevLett.114.175002
- Wan, M., Matthaeus, W. H., Roytershteyn, V., Parashar, T. N., Wu, P., and Karimabadi, H. (2016). Intermittency, coherent structures and dissipation in plasma turbulence. *Phys. Plasmas* 23, 042307. doi:10.1063/1.4945631
- Wu, P., Perri, S., Osman, K., Wan, M., Matthaeus, W. H., Shay, M. A., et al. (2013). Intermittent Heating in Solar Wind and Kinetic Simulations. *Astrophys. J. Lett.* 763, L30. doi:10.1088/2041-8205/763/2/L30
- Zhao, G. Q., Feng, H. Q., Wu, D. J., Liu, Q., Zhao, Y., Zhao, A., et al. (2018). Statistical Study of Low-Frequency Electromagnetic Cyclotron Waves in the Solar Wind at 1 AU. *J. Geophys. Res.* 123, 1715–1730. doi:10.1002/2017JA024979
- Zhao, J. S., Voitenko, Y. M., Wu, D. J., and Yu, M. Y. (2016). Kinetic Alfvén turbulence below and above ion cyclotron frequency. *J. Geophys. Res.* 121, 5–18. doi:10.1002/2015JA021959
- Zhdankin, V., Uzdensky, D. A., Werner, G. R., and Begelman, M. C. (2019). Electron and Ion Energization in Relativistic Plasma Turbulence. *Phys. Rev. Lett.* 122, 055101. doi:10.1103/PhysRevLett.122.055101